

# MPC-Based Voltage/Var Optimization for Distribution Circuits With Distributed Generators and Exponential Load Models

Zhaoyu Wang, *Student Member, IEEE*, Jianhui Wang, *Senior Member, IEEE*, Bokan Chen, Miroslav M. Begovic, *Fellow, IEEE*, and Yanyi He

**Abstract**—This paper proposes a model predictive control (MPC)-based voltage/var optimization (VVO) technique considering the integration of distributed generators and load-to-voltage sensitivities. The paper schedules optimal tap positions of on-load tap changer and switch statuses of capacitor banks based on predictive outputs of wind turbines and photovoltaic generators. Compared with previous efforts on VVO which used constant-power load model, the exponential load model is used to capture the various load behaviors in this paper. Different customer types such as industrial, residential, and commercial loads are also considered. The uncertainties of model prediction errors are taken into account in the proposed model. A scenario reduction technique is applied to enhance a tradeoff between the accuracy of the solution and the computational burden. The MPC-based VVO problem is formulated as a mixed-integer nonlinear program with reduced scenarios. Case studies show the effectiveness of the proposed method.

**Index Terms**—Distributed generators, exponential load model, mixed-integer program, model predictive control, scenario reduction, voltage/var optimization.

## NOMENCLATURE

$B$	Set of nodes in the distribution system.
$S$	Set of initial scenarios.
$J$	Set of scenarios to be deleted.
$P_i$	Active power flow from node $i$ to $i + 1$ .
$Q_i$	Reactive power flow from node $i$ to $i + 1$ .
$V_i$	Voltage at node $i$ .

Manuscript received August 3, 2013; revised November 9, 2013 and February 9, 2014; accepted April 30, 2014. Date of current version September 5, 2014. This work was supported in part by UChicago Argonne, LLC, Operator of Argonne National Laboratory Argonne, a U.S. Department of Energy Office of Science laboratory under Contract DE AC02-06CH11357, and in part by the U.S. Department of Energy Office of Electricity Delivery and Energy Reliability. The U.S. Government retains for itself, and others acting on its behalf, a paid-up nonexclusive irrevocable worldwide license in said article to reproduce, prepare derivative works, distribute copies to the public, and perform publicly and display publicly, by or on behalf of the Government. Paper no. TSG-00584-2013.

Z. Wang and M. M. Begovic are with the School of Electrical and Computer Engineering, Georgia Institute of Technology, Atlanta, GA 30332 USA (e-mail: zhaoyuwang@gatech.edu; miroslav@ece.gatech.edu).

J. Wang is with the Argonne National Laboratory, Lemont, IL 60439 USA (e-mail: jianhui.wang@anl.gov).

B. Chen and Y. He are with the School of Industrial and Manufacturing Systems Engineering, Iowa State University, Ames, IA 50014 USA (e-mail: bokanc@iastate.edu; heyanyi@iastate.edu).

Color versions of one or more of the figures in this paper are available online at <http://ieeexplore.ieee.org>.

Digital Object Identifier 10.1109/TSG.2014.2329842

$p_i^l$	Active load consumption at node $i$ .
$q_i^l$	Reactive load consumption at node $i$ .
$p_i^g$	Active power generation at node $i$ .
$q_i^g$	Reactive power generation at node $i$ .
$r_i + jx_i$	Impedance of the line between nodes $i$ and $i + 1$ .
$\ell$	Active power losses of the distribution system.
$\Delta V_{i,t}$	Voltage deviation of node $i$ from the first node at time $t$ .
$\varepsilon$	Maximum allowable voltage deviation.
$k_{pi}$	Active power exponent for the exponential load model at node $i$ .
$k_{qi}$	Reactive power exponent for the exponential load model at node $i$ .
$P_{i,t}^{b,pred}$	Predicted active load component at nominal voltage for the exponential load model at node $i$ and time $t$ .
$Q_{i,t}^{b,pred}$	Predicted reactive load component at nominal voltage for the exponential load model at node $i$ and time $t$ .
$M_t^p$	Multiplier for active load at time $t$ .
$M_t^q$	Multiplier for reactive load at time $t$ .
$T_p$	Prediction horizon in MPC.
$T_c$	Control horizon in MPC.
$t_k$	Discrete time instant of MPC.
$TAP_t$	Tap position of OLTC during time interval $t$ .
$TAP^{\max}$	Maximum number of OLTC operations during time $t$ to time $t + T_p$ .
$c_{i,t}$	Binary indicator of the switch status of the capacitor at node $i$ during at time $t$ (1-ON, 0-OFF).
$Q_i^{cap}$	Size of the capacitor at node $i$ .
$CAP^{\max}$	Maximum switch times of capacitors during time $t$ to time $t + T_p$ .
$a_{i,t}$	$a_{i,t} = c_{i,t}c_{i,t+T_c}$ .
$s_{i,t}$	Binary indicator for switch status change of the capacitor at node $i$ from time $t$ to $t + T_c$ .
$\varphi_t$	Integer represents tap changes of the OLTC from time $t$ to $t + T_c$ .
$\omega_t$	Scenario set of prediction errors at time $t$ , $\omega_t = \left\{ \omega_t^j \right\}_{j=1, \dots, N}$ .
$P_{i,t}^{pred}$	Predicted output of the DG at node $i$ and time $t$ .
$S_{base}$	Power base for the system.
$\alpha_{i,t}, \beta_{i,t}$	Shape parameters of Beta function.
$\sigma_{i,t}$	Standard deviation of the prediction error.

$N$	Number of initial scenarios.
$n$	Number of reduced scenarios.
$\omega_t^s$	Prediction error in scenario $s$ at time $t$ .
$\rho_s$	Original probability of scenario $s$ .
$\rho'_s$	Aggregated probability of scenario $s$ .

## I. INTRODUCTION

**V**OLTAGE and var optimization (VVO) is a secondary control scheme to the daily operation of distribution systems. VVO is achieved by on-load tap changers (OLTCs) and var compensation devices such as capacitors. The main purpose of VVO is to coordinate the schedules of tap positions of OLTCs and statuses of switched capacitors to improve the power quality and operations of distribution systems. The increasing penetration of distributed generators (DGs) has great impacts on conventional VVO due to the uncertain outputs of renewable energy sources (RES)-based DGs [1], [2].

Many papers in the literature have investigated the VVO problem in distribution networks [3]–[7]. Reference [3] treated the regulation of OLTC and capacitors as two decoupled problems and provided an optimal real-time control scheme. Reference [4] studied the coordination of voltage regulators and capacitors. A multiobjective genetic algorithm (GA) was used to deal with the integrated VVO so as to minimize power losses and voltage deviations. In [5], OLTC and capacitors were dispatched hourly based on day-ahead load forecast. Reference [6] proposed a two-stage coordinated control between OLTC and capacitor banks (CBs). The dispatch schedules of CBs were generated using a heuristic algorithm based on the forecasted load, and the OLTC was controlled in real time. Reference [7] presented an artificial neural network (ANN)-based optimal coordination control scheme for OLTC and STATCOM in a distribution system. However, the existence of DGs was not considered in these papers.

As the penetration level of DGs grows, their impacts on voltage and reactive power in distribution systems have attracted more and more attention [8]. The outputs of RES-based DGs can be highly stochastic. Meanwhile, the value of resistance can be close to that of reactance in a distribution circuit, which highlights impacts of DG outputs on VVO [1]. Reference [9] investigated the coordination of OLTC and capacitors to minimize power losses in a distribution system with DGs. The DGs were assumed to be synchronous machine-based ones whose outputs were controllable. Reference [10] proposed a combined centralized and local control scheme for VVO to minimize losses in the presence of induction machine-based DGs. Loads were assumed to be constant power loads. It was also assumed that the wind power can be forecasted without errors. Reference [11] proposed an optimal control of distribution voltages with the coordination of voltage regulators, capacitors, shunt reactors and static var compensators (SVCs) in a distribution system with photovoltaic (PV) generation. However, the output of PV was assumed to be known. Reference [12] proposed an optimal reactive power coordination strategy to minimize the number of tap operations of line voltage regulators in distribution systems with high PV penetration. Reference [13] proposed a hybrid voltage/var control

for a distribution system with PV generation. There are only a few papers considering the stochastic nature of RES-based DGs in solving the VVO problem. Reference [1] applied a teaching-learning algorithm (TLA) to schedule VVO dispatch, the stochastic outputs of DGs were converted to a series of equivalent deterministic scenarios. The study in [14] used GA for optimal var control considering wind farms to minimize system losses.

All of the above literature ignores the load-to-voltage (LTV) relationship and use constant-power models to represent load behaviors, which may not be accurate in practice [15]. Load models have significant impacts on power system operation and analysis [16], [17]. The studies of power system stability, operation, and planning strongly depend on the accuracy of load models and their parameters. The conventional constant-power load models which are normally used in previous studies assume that the load is insensitive to voltage, which may not be realistic and lead to inaccurate VVO dispatches. This is especially true in distribution systems since the LTV sensitivities may vary from one node to another due to the complicated load compositions. The LTV will greatly impact the effectiveness of VVO. Meanwhile, the ever-increasing penetration of DGs has introduced additional constraints and uncertainties into the voltage control of power systems. The voltage control of power systems is a multiobjective optimization problem that requires more effective and robust control strategies [18]. The control strategies based on prediction of system behaviors are receiving more interest due to the flexibility of online optimization in explicitly incorporating voltage control specifications and operational constraints; such methods are usually referred to as model predictive control (MPC).

MPC has been applied in power system operations and controls [19]. Reference [20] applied MPC in voltage coordination of multiarea power systems. Reference [21] used a centralized MPC and a heuristic algorithm to coordinate generator voltage set-points, LTC, and load shedding. Reference [22] employed MPC to select a combination of shunt capacitors, load shedding, and generator voltage set-points to correct non-viable transmission voltages. However, the stochastic nature of model prediction errors was not considered in these papers.

This paper proposes a MPC-based formulation for the optimal dispatch of OLTC and CBs considering the load models and the uncertainty of DG outputs. The exponential load model is used to represent LTV relationships. A practical distribution system may consist of various types of customers such as residential, commercial and industrial loads. Thus, each type of customer is assigned with assumed exponents in the exponential load models [23]. The uncertainties of prediction errors in the MPC-based VVO are taken into account using a scenario-based approach. The probabilistic prediction errors result from the integration of RES-based DGs (wind turbines and PVs). Monte-Carlo simulations are used to generate scenarios. The simultaneous backward scenario reduction method [24] is applied to increase the calculation speed while maintaining the accuracy of the solution. The MPC-based VVO problem is formulated as a mixed-integer nonlinear program (MINLP) with reduced scenarios and then solved by

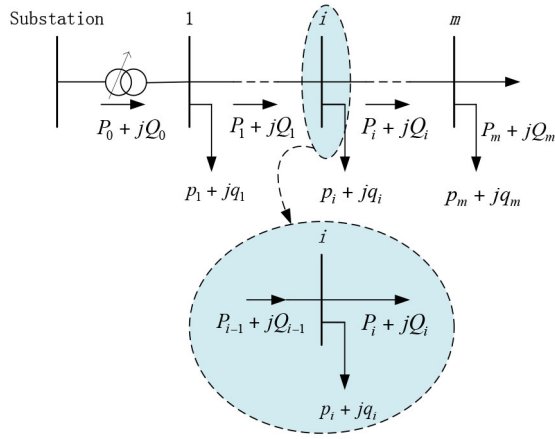


Fig. 1. Schematic diagram of a radial distribution system.

GAMS/DICOPT [25]. Case studies show that load models and probabilistic prediction errors of DG outputs can significantly impact the optimal VVO schedule.

The remainder of this paper is organized as follows. Section II introduces the distribution system, load models, and MPC theory as well as the mathematical formulation of the stochastic MPC-based VVO problem. Section III introduces scenario generation and reduction for the problem. Section IV provides case studies to show the effectiveness of the proposed method. Section V concludes the paper with major findings.

## II. MPC-BASED VOLTAGE/VAR CONTROL

### A. Distribution System Model

Consider a distribution system as shown in Fig. 1, there are  $m$  buses indexed by  $i = 0, 1, \dots, m$ . The following equations can be used to describe the complex power flows at each node  $i$  [26], [27]:

$$P_{i+1} = P_i - r_i \frac{P_i^2 + Q_i^2}{V_i^2} - p_{i+1} \quad (1)$$

$$Q_{i+1} = Q_i - x_i \frac{P_i^2 + Q_i^2}{V_i^2} - q_{i+1} \quad (2)$$

$$V_{i+1}^2 = V_i^2 - 2(r_i P_i + x_i Q_i) + (r_i^2 + x_i^2) \frac{P_i^2 + Q_i^2}{V_i^2} \quad (3)$$

$$p_i = p_i^l - p_i^g, \quad q_i = q_i^l - q_i^g. \quad (4)$$

In this paper, we assume that  $p_i^g$  is generated by DG units at node  $i$ ,  $q_i^g$  is generated by VAR compensation devices which are capacitors.  $q_i^g$  can be negative if DGs draw reactive power from the distribution system.

### B. Load Models

Many load models have been developed in the past, among which, exponential load model (ELM) is widely used to represent LTV relationship [23]. The ELM is defined as

$$p_i^l = P_i^b V_i^{k_{pi}} \quad (5)$$

$$q_i^l = Q_i^b V_i^{k_{qi}}. \quad (6)$$

TABLE I  
LOAD TYPES AND EXPONENT VALUES

Load Type	$k_p$	$k_q$
Residential	1.04	4.19
Commercial	1.50	3.15
Industrial	0.18	6.00

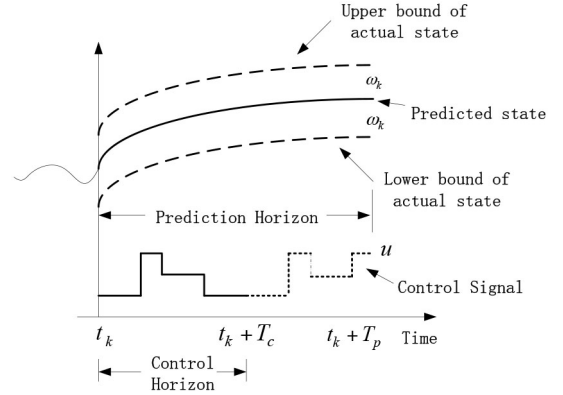


Fig. 2. Demonstration of MPC.

In the constant power load model,  $k_{pi}$  and  $k_{qi}$  are assumed to be zero. In fact, the exponents  $k_{pi}$  and  $k_{qi}$  are related with load compositions. Table I shows the example exponent values for different types of loads [23], which will be used in this paper for illustration. In practice, a feeder is not explicitly residential, commercial or industrial [17]. Thus, a load class mix will be implemented; the details are discussed in Section IV.

### C. Model Predictive Control

MPC refers to algorithms that solve a finite-horizon optimal control problem over the prediction horizon  $T_p$ , the obtained control variables are applied to the system over the control horizon  $T_c$  ( $T_c \leq T_p$ ). At the end of the control horizon, the rest of the predicted control variables are discarded and the entire procedure is repeated [20]. Fig. 2 demonstrates the processes of MPC. At a discrete time instant  $t_k$ , the future system behavior is predicted over a finite window  $[t_k, \dots, t_k + T_p]$ . The optimal control problem is solved based on the prediction data to obtain a sequence of control signals  $[u(t_k), u(t_{k+1}), \dots, u(t_k + T_p)]$ . The control signals beyond  $t_k + T_c$  will be discarded (shown in dotted line) and others will be implemented into the system (shown in bold line). The above process is repeated using new observations at  $t_{k+1}$ . In this paper, we assume  $T_c = t_{k+1} - t_k$  [20].

In practice, the prediction errors  $\omega$  should be considered, especially when highly variable components such as DGs exist in the system. The details on prediction errors of MPC will be discussed in Section III.

### D. Mathematical Formulation of MPC

Consider using power losses of the distribution system and voltage deviations along the feeder as control objectives, the

multiobjective VVO problem for a certain control period can be formulated as follows:

$$\min \mathbb{E} \left[ \sum_{t=t_k}^{t_k+T_p} (\ell_t(\omega_t) + \Delta V_t(\omega_t)) \right] \quad (7)$$

subject to

$$\begin{aligned} \Delta V_t(\omega_t) &= \max_i \{ \Delta V_{i,t}(\omega_t) \}, \quad \Delta V_{i,t}(\omega_t) \\ &= |V_{i,t}(\omega_t) - V_{1,t}(\omega_t)| \end{aligned} \quad (8)$$

$$\ell_t(\omega_t) = \sum_i r_i \frac{P_{i,t}^2(\omega_t) + Q_{i,t}^2(\omega_t)}{V_{1,t}^2(\omega_t)}, \quad \forall i \in B \quad (9)$$

$$P_{i+1,t}(\omega_t) = P_{i,t}(\omega_t) - p_{i+1,t}(\omega_t) \quad (10)$$

$$Q_{i+1,t}(\omega_t) = Q_{i,t}(\omega_t) - q_{i+1,t}(\omega_t) \quad (11)$$

$$V_{i+1,t}(\omega_t) = V_{i,t}(\omega_t) - \frac{r_i P_{i,t}(\omega_t) + x_i Q_{i,t}(\omega_t)}{V_{1,t}(\omega_t)} \quad (12)$$

$$p_{i,t}(\omega_t) = p_{i,t}^l - p_{i,t}^g(\omega_t) \quad (13)$$

$$q_{i,t}(\omega_t) = q_{i,t}^l - q_{i,t}^g(\omega_t) \quad (14)$$

$$p_{i,t}^g(\omega_t) = P_{i,t}^{pred} + \omega_{i,t} \quad (15)$$

$$q_{i,t}^g = c_{i,t} Q_i^{cap} \quad (16)$$

$$V_{1,t} = TAP_t V_s \quad (17)$$

$$p_{i,t}^l = \left( P_{i,t}^{b,pred} + \omega_t \right) V_{i,t}^{k_{pi}}(\omega_t) \quad (18)$$

$$q_{i,t}^l = \left( Q_{i,t}^{b,pred} + \omega_t \right) V_{i,t}^{k_{qi}}(\omega_t) \quad (19)$$

$$1 - \varepsilon \leq V_{i,t}(\omega_t) \leq 1 + \varepsilon \quad (20)$$

$$\sum_{t=t_k}^{t_k+T_p-T_c} |c_{i,t+T_c} - c_{i,t}| \leq CAP^{\max} \quad (21a)$$

$$\sum_{t=t_k}^{t_k+T_p-T_c} |TAP_{t+T_c} - TAP_t| \leq TAP^{\max}. \quad (21b)$$

In the above formulation, the objective function (7) minimizes the expectation of active power losses and voltage deviations along the feeder during the prediction horizon. For illustration, we assume the two objectives are equally weighted. However, the distribution system operators (DSOs) can change the weighting factors (priorities) according to the specific operational requirements. Equation (8) represents the maximum voltage deviation of all nodes. Equation (9) describes active power losses of the distribution network. Equations (10)–(12) are the linear form of the DistFlow equations defined in (1)–(4), which have been extensively verified and used in the literature [26]–[29]. The linearization is based on the fact that the nonlinear terms in (1)–(4) are much smaller than the linear terms [29], [30]. The outputs of DG units and capacitors are represented as negative loads in constraints (13)–(14). Equation (15) assumes outputs of DG units equal the predicted values plus the predicted errors  $\omega$ .  $\omega$  belongs to an uncertainty set, which may vary with predicted values and will be discussed in next section. In constraint (16),  $c_{i,t}$  represents the on/off status of the capacitor at node  $i$  during the time interval  $t$ . For nodes without capacitors,  $Q_i^{cap}$  equals zero. In constraint (17),  $V_s$  represents the primary voltage of the transformer at the substation, which is assumed to be

1.0 p.u. in this paper. The secondary voltage is modeled as a function of the primary voltage [3], [4]. The detailed model can be found in [4]. Voltage regulators (VRs) are voltage control devices often used on long lines and can participate in VVO. A single-phase VR with an open-delta configuration, 32 taps ( $[-16, \dots, +16]$ ) and  $\pm 10\%$  tap range can be modeled as follows [4]:

$$V_{i,t} = V_r \sqrt{1 + 3(TAP_{i,t}/16) + 3(TAP_{i,t}/16)^2} \quad (22)$$

where  $V_r$  is the input voltage of the VR,  $TAP_{i,t}$  represents the tap position of the VR of node  $i$  at time  $t$ . Equation (22) can be integrated into the VVO formulation when VRs exist in the distribution system.

Constraints (18) and (19) use the exponential load model to represent active and reactive load consumptions.  $P_{i,t}^{b,pred}$  and  $Q_{i,t}^{b,pred}$  change with a load profile which can be obtained by using short-term load forecasting techniques. Constraint (20) indicates the voltage of each node should be within a certain range for proper operation of the distribution circuit,  $\varepsilon$  is usually set to be 0.05. Constraints (21a) and (21b) describe the max. number of daily switching operations of OLTC and capacitors, respectively. In some practical cases, a bank of capacitors may be installed at node  $i$ . Then, the discrete output of the CB at node  $i$  can be represented as (23a) and constraint (21a) can be modified accordingly as shown in (23b).

$$q_{i,t}^g = \sum_k c_{i,k,t} Q_{ik}^{cap} \quad (23a)$$

$$\sum_{t=t_k}^{t_k+T_p-T_c} |c_{i,k,t+T_c} - c_{i,k,t}| \leq CAP^{\max} \quad (23b)$$

where  $c_{i,k}$  is a binary indicator of the switch status of the  $k$ th capacitor in the CB at node  $i$  and  $Q_{ik}^{cap}$  represents the size of the  $k$ th capacitor in the CB at node  $i$ . This paper considers the case that one capacitor is installed at one node. However, it is clear that the proposed method can be applied to solve the VVO problem with CBs. The maximum number of daily switching operations of OLTC and capacitors should be less than the predefined values. For illustration,  $CAP^{\max}$  is set to be 3 and  $TAP^{\max}$  is set to be 5 in this paper. The DSOs can change these settings according to the characteristics of a specific system. To further reduce the nonlinearity of the above problem, some constraints can be reformulated. Equation (8) can be reformulated as follows:

$$\lambda_t(\omega_t) \geq V_{i,t}(\omega_t) - V_{0,t}(\omega_t), \quad \forall i \in B \quad (24a)$$

$$\lambda_t(\omega_t) \geq V_{0,t}(\omega_t) - V_{i,t}(\omega_t), \quad \forall i \in B. \quad (24b)$$

In constraint (21), assume  $s_{i,t} = (c_{i,t+T_c} - c_{i,t})^2$ , since  $c_{i,t}$  is a binary,  $c_{i,t}^2 = c_{i,t}$ , we have

$$s_{i,t} = c_{i,t+T_c} + c_{i,t} - 2c_{i,t+T_c}c_{i,t}. \quad (25)$$

$s_{i,t}$  indicates whether the capacitor at node  $i$  has changed its status from time  $t$  to time  $t + T_c$  ( $s_{i,t} = 1$ , if the status has changed). To linearize the multiplication of  $c_{i,t+T_c}c_{i,t}$ , we

TABLE II  
RELATIONSHIP AMONG  $s_{i,t}$ ,  $a_{i,t}$ , AND  $c_{i,t}$

$s_{i,t}$	$a_{i,t}$	$c_{i,t+\Delta t}$	$c_{i,t}$
0	0	0	0
0	1	1	1
1	0	0	1
1	0	1	0

denote  $a_{i,t} = c_{i,t+T_c}c_{i,t}$ , and  $a_{i,t}$  is a binary. Equation (25) can be represented as

$$s_{i,t} = c_{i,t+T_c} + c_{i,t} - 2a_{i,t} \quad (26)$$

$$a_{i,t} \leq c_{i,t}, a_{i,t} \leq c_{i,t+T_c}, a_{i,t} \geq c_{i,t} + c_{i,t+T_c} - 1. \quad (27)$$

Table II illustrates the effectiveness of (26) and (27). It can be seen that  $s_{i,t}$  can represent the switch status of the capacitor. The constraint (21a) can be reformulated as a linear constraint

$$\sum_{t=t_k}^{t_k+T_p-T_c} s_{i,t} = \sum_{t=t_k}^{t_k+T_p-T_c} (c_{i,t+T_c} + c_{i,t} - 2a_{i,t}) \leq CAP^{\max}. \quad (28)$$

In constraints (21b),  $TAP_t$  is an integer whose range is dependent on the number of taps of the OLTC. Equation (22) can be reformulated as follows:

$$\varphi_t \geq TAP_{t+T_c} - TAP_t \quad (29)$$

$$\varphi_t \geq TAP_t - TAP_{t+T_c} \quad (30)$$

$$\sum_{t=t_k}^{t_k+T_p-T_c} \varphi_t \leq TAP^{\max}. \quad (31)$$

The stochastic optimization problem can be represented as follows:

$$\begin{aligned} \min \mathbb{E} \left[ \sum_{t=t_k}^{t_k+T_p} (\ell_t(\omega_t) + \lambda(\omega_t)) \right] \\ \text{s.t. (9)–(20), (24)–(31)} \end{aligned} \quad (32)$$

### III. SOLUTION METHODOLOGY

#### A. Prediction Error and Scenario Generation

In this paper, two kinds of DGs are considered: wind turbines and PVs, the predicted wind and solar power will be used. It is known that errors always exist in prediction models. The normal distribution and beta distribution are used by previous papers to represent the wind power prediction errors [31], [32]. It has been shown that the beta function is more appropriate than the standard normal distribution in representing prediction errors of wind power [31], [33]. The prediction errors of solar power are still under study. In [1], the beta function has also been used in representing the prediction errors of solar power. Since the purpose of this paper is to calculate dispatches of VVO devices based on predicted DG outputs, each prediction horizon corresponds to two beta functions for prediction errors: one for wind power and the other for solar power.

For a predicted power  $P_{i,t}^{pred}$ , the beta function can be defined by two corresponding parameters  $\alpha$  and  $\beta$  [33]

$$f_{P_{i,t}^{pred}}(x) = x^{\alpha-1}(1-x)^{\beta-1}. \quad (33)$$

The above beta function models the occurrence of real power values  $x$  when a certain prediction value  $P_{i,t}^{pred}$  has been forecasted. Shape parameters  $\alpha$  and  $\beta$  can be calculated as

$$\frac{P_{i,t}^{pred}}{S_{base}} = \frac{\alpha_{i,t}}{\alpha_{i,t} + \beta_{i,t}} \quad (34)$$

$$\sigma_{i,t}^2 = \frac{\alpha_{i,t}\beta_{i,t}}{(\alpha_{i,t} + \beta_{i,t})^2(\alpha_{i,t} + \beta_{i,t} + 1)}. \quad (35)$$

The relationship between the predicted power and its error variance can be represented as [1], [33]

$$\sigma_{i,t} = 0.2 \times \frac{P_{i,t}^{pred}}{P_i^{cap}} + 0.21. \quad (36)$$

Using the predicted DG outputs and the (34)–(36), the parameters of beta functions for the current prediction horizon can be calculated. A normal distribution is frequently used to represent the forecasting uncertainty of load consumptions, in which, the mean value of the normal distribution is the forecasted load and the stand deviation is set to be 2% of the expected load [34]. Monte-Carlo simulation (MCs) is run based on forecasted power and uncertain prediction errors to generate scenarios for DG outputs and load consumptions. All of the above distributions and parameters settings can be changed according to the available information of a system.

#### B. Scenario Reduction

In order to reduce the computation efforts, a scenario reduction technique is implemented to reduce the number of scenarios while maintaining a good approximation of the system uncertainty. In this paper, the simultaneous backward reduction method [24] will be used for scenario reduction. Let  $\tau_s (s = 1, \dots, N)$  denote  $N$  different scenarios, each with a probability of  $\rho_s$ , we define a distance function  $d(\tau_s, \tau_{s'})$  for the scenario pair  $(\tau_s, \tau_{s'})$

$$d(\tau_s, \tau_{s'}) := \max\{1, \|\tau_s - \bar{\tau}\|, \|\tau_{s'} - \bar{\tau}\|\} \|\tau_s - \tau_{s'}\| \quad (37)$$

where  $\bar{\tau}$  is the average value of scenarios. Denote  $S$  as the initial set of scenarios ( $N$  initial elements) and  $J$  (initially null) as the set of scenarios to be deleted. Assume there are  $N$  scenarios and we would like to reduce them into  $n$  scenarios. The steps can be summarized as follows.

*Step 1:* Compute the distances of all scenario pairs  $d_{s,s'} = d(\tau_s, \tau_{s'}) (s, s' = 1, \dots, N)$ . For each scenario  $l$ ,  $\phi_l^{[1]} := \min_{j \neq l} d_{l,j} (j = 1, \dots, N)$ , let  $l_1 \in \arg \min_{l \in \{1, \dots, N\}} \rho_l \phi_l^{[1]}$ , we can obtain the first element of  $J$ ,  $J^{[1]} = \{l_1\}$  and  $S$  is updated by  $S^{[1]} = S / \{l_1\}$ .

*Step  $i$  ( $i > 1$ ):* For each scenario  $l$ ,  $l \in S^{[i-1]}$ , compute  $\phi_{kl}^{[i]} := \min_{k' \in J^{[i-1]} \cup \{l\}} d_{k,k'}$ ,  $k \in J^{[i-1]} \cup \{l\}$ , then compute  $z_l^{[i]} := \sum_{k \in J^{[i-1]} \cup \{l\}} \rho_k \phi_{kl}^{[i]}$ , let  $l_i \in \arg \min z_l^{[i]}$ , update  $J$  and  $S$  by  $J^{[i]} = J^{[i-1]} \cup \{l_i\}$ ,  $S^i = S^{i-1} / \{l_i\}$ , repeat this step for  $N - n$  times.

*Step  $N - n + 1$ :* After obtaining the final  $J$  set (with  $N$  elements) and the  $S$  set (with  $n$  elements), for the each remaining scenario  $s \in S$ , its new probability  $\rho'_s$  can be calculated as

$$\rho'_s = \rho_s + \sum_{j \in J_j} \rho_j \quad (38)$$

where  $J_j$  can be calculated as follows: for each  $j \in J$ ,  $J_j = \{\psi | \psi \in \arg \min_{h \in J} d(\tau_h, \tau_j)\}$ .

The number of scenarios can be reduced from  $N$  to  $n$  through the above procedures. The problem defined in (32) can be reformulated using the reduced scenarios as follows:

$$\begin{aligned} \min \sum_{s=1}^n \rho'_s [\sum_{t=t_k}^{t_k+T_p} (\ell_t(\omega_t^s) + \lambda(\omega_t^s))] \\ \text{s.t. (9)–(20), (24)–(31)} \end{aligned} \quad (39)$$

The problem is MINLP, which can be solved by commercial solvers, such as DICOPT [25]. The above formulation schedules the dispatches of VVO devices for the current prediction horizon based on predicted DG outputs so as to minimize active power losses and voltage deviations. The process is repeated when new observations come at  $t_{k+1}$ . DG outputs can be predicted by regression-based methods or machine learning-based techniques, which are beyond the contents of this paper. The comprehensive procedure for MPC-based VVO can be summarized as (start from  $t = t_k$ ).

- Step 1: Predict DG outputs for the time period  $[t, t + T_p]$ .
- Step 2: Calculate corresponding beta functions for the predicted DG outputs; obtain  $N$  scenarios of prediction errors using MCs; reduce the number of scenarios to  $n$ .
- Step 3: Solve the MINLP problem in (38) and obtain the VVO schedule for the time period  $[t, t + T_p]$ .
- Step 4: Implement the VVO schedule for the time period  $[t, t + T_c]$ . When  $t = t_k + T_c = t_{k+1}$ , go to step 1.

It is necessary to show how much improvement can be achieved if the stochastic prediction errors are taken into account in MPC. We define the solution of (39) as  $\hat{x}$ . For the problem defined in (32), we replace the random error  $\omega$  by its expected value, and then the expected value problem (EV), which is a deterministic optimization problem, can be defined as

$$EV = \min \sum_{t=t_k}^{t_k+T_p} (\ell_t(\bar{\omega}_t) + \lambda(\bar{\omega}_t)) \quad (40)$$

where  $\bar{\omega}_t = E(\omega_t)$  denotes the expectation of  $\omega_t$ . The expected value solution can be defined as  $\bar{x}$ . The expected results of using the EV solution can be represented as

$$EEV = \frac{1}{N'} \sum_{h=1}^{N'} (\ell_t(\bar{x}, \omega^h) + \lambda(\bar{x}, \omega^h)). \quad (41)$$

EEV measures the performance of  $\bar{x}$ , allowing second-stage decision variables to be chosen optimally as functions of  $\bar{x}$  and  $\omega$ . The  $N'$  scenarios of prediction errors are generated by MCs. We can compare EEV and the objective value of (39) to see how the stochastic programming outperforms the deterministic programming.

#### IV. CASE STUDY

The proposed methodology has been examined on the modified IEEE 33-bus radial distribution network as shown in Fig. 3. Details about the test system can be found in [26]. Assume the substation transformer is with  $\pm 10\%$  tap range. Switched capacitors are installed at nodes 2, 3, 6, 11, 21

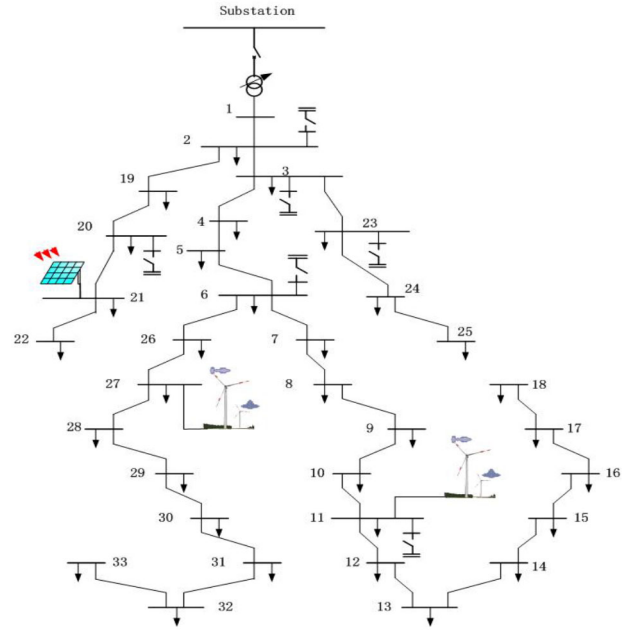


Fig. 3. Test distribution system.

TABLE III  
NODE TYPES

Type	Residential	Commercial	Industrial
Node number	2, 3, 4, 5, 6, 7, 8, 9, 12, 13, 14, 15	10, 11, 16, 17, 19, 20, 21, 22	18, 23, 24, 25

and 23, each is 30 kvar. PV panels are installed at node 21, wind turbines are located at nodes 11 and 27. The node types are listed in Table III. In this example, we set  $T_p$  to be 6 h,  $T_c$  to be 15 min. For every 15 min, the MPC predicts the DG outputs and load consumptions for the next 6 h and makes control decisions. 100 scenarios ( $N = 100$ ) are generated using Monte-Carlo simulation to represent the prediction errors in the prediction horizon. As discussed in the previous section, scenario reduction is applied to reduce the computation efforts while maintaining the solution accuracy. The 100 generated scenarios are reduced to 15 scenarios ( $n = 15$ ) in this case. The above procedure is repeated for the whole day.

All loads are represented by ELM, the load consumption of node  $i$  at time  $t$  can be represented as

$$p_{i,t}^l = P_i^b M_i^p V_{i,t}^{k_{pi}} \quad (42)$$

$$q_{i,t}^l = Q_i^b M_i^q V_{i,t}^{k_{qi}}. \quad (43)$$

The values of basic components  $P_i^b$  and  $Q_i^b$  can be found in [26], the exponents of each type of load are shown in Table I. The multipliers  $M_i^p$  and  $M_i^q$ , as shown in Fig. 4, are used to make the load profile change with time. It is assumed that multipliers of all nodes are the same.

Fig. 5 shows the normalized predicted wind and solar power that will be used in this paper. The power base of the system  $S_{base}$  is set to be 1 MVA.

The stochastic VVO problem defined in (39) is solved with the 15 scenarios for every prediction horizon. Fig. 6 shows the daily optimal dispatch of OLTC tap positions, in which, Tap

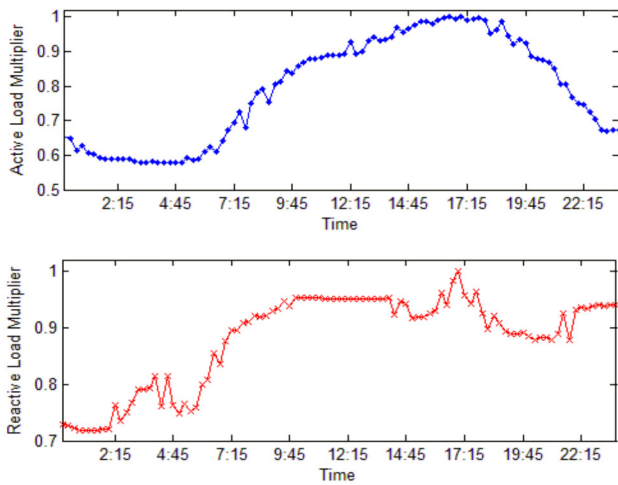


Fig. 4. Load shape multipliers.

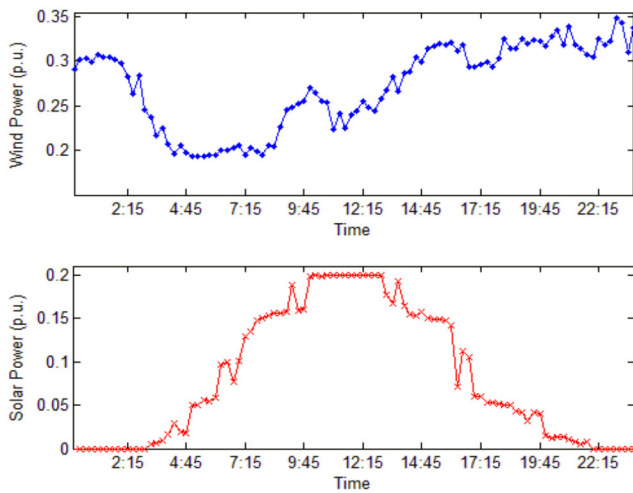


Fig. 5. Predicted wind and solar power.

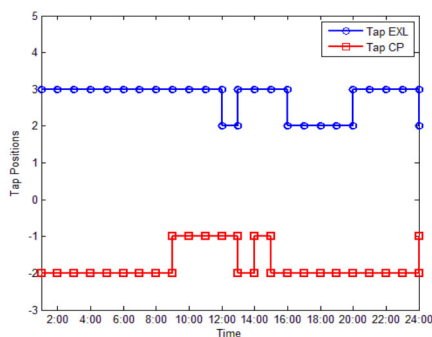


Fig. 6. Tap positions with exponential model and constant power model.

EXL refers to tap positions with ELM and Tap CP refers to tap positions with the constant-power model. It can be seen that the optimal taps of OLTC are quite different for ELM and the constant-power model.

Figs. 7–9 show the switch statuses of capacitors, where EXL represents the results with the ELM, CP represents the results with the constant-power load model. It can be seen that

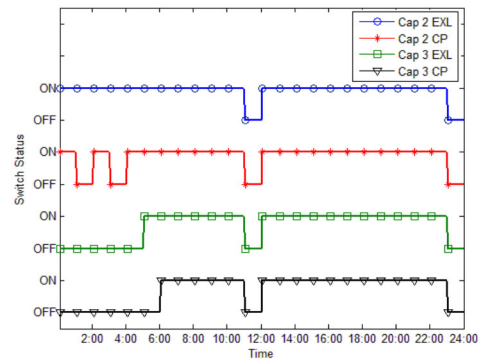


Fig. 7. Switch statuses of capacitor 2 and 3 with exponential model and constant power model.

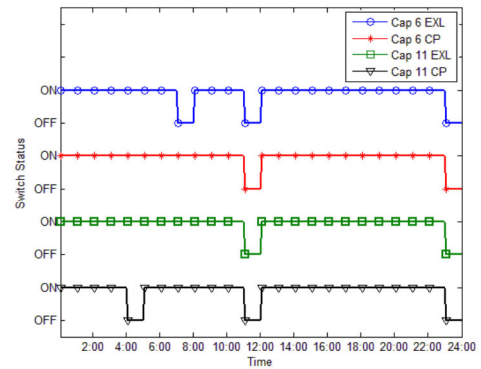


Fig. 8. Switch statuses of capacitor 6 and 11 with exponential model and constant power model.

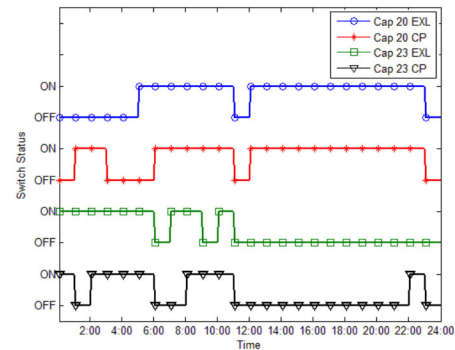


Fig. 9. Switch statuses of capacitor 20 and 23 with exponential model and constant power model.

daily dispatches of most capacitors change with different load models (capacitor at node 3 does not change).

Fig. 10 shows the voltages of all nodes. Voltage levels at 6:00, 12:00, 18:00, and 24:00 are selected to be shown due to the space limit. EXL represents the voltages with the ELM, CP represents the voltages with the constant-power load model and Base represents the voltages with DGs and ELM, but without OLTC or capacitors. Compared with the base case, the proposed stochastic VVO method considering DGs can largely improve the voltage profile no matter which kind of load models is used. All the voltages are within 0.95 to 1.05 p.u., which satisfies the voltage constraint. The optimal voltage levels with the constant-power load model are relatively higher than those

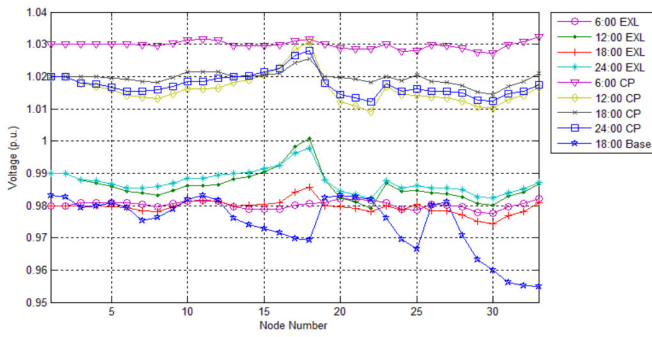


Fig. 10. Voltage profiles.

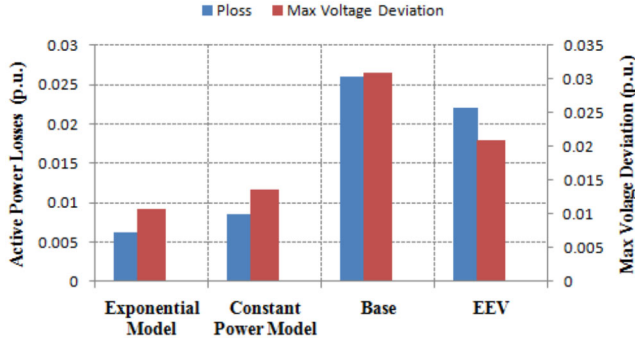


Fig. 11. Active power losses and max voltage deviations.

with ELM. The reason is that losses are proportional to the square of the current, and the current of a constant-power load is inversely proportional to the voltage [10]. Thus, the OLTC will operate the feeder in the upper bound of the allowable voltage range to reduce losses.

Fig. 11 shows the active power losses and maximum voltage deviation of VVO with ELM, constant-power load model, EEV, and the base case without VVO. It can be seen that the MPC-based VVO method can improve the system operation. For example, compared with the base case with DGs and without VVO, the MPC-based VVO with ELM reduces the maximum voltage deviation by 65%, and power losses by 77%. Compared with the deterministic MPC (labeled as EEV in Fig. 11), the proposed stochastic MPC considering prediction errors and ELM (labeled as exponential model in Fig. 11) can reduce the maximum voltage deviation by 49% and power losses by 72%. Meanwhile, the objective function values of systems with ELM and the constant-power model are different. Since loads are sensitive to voltage in practice and different types of loads may have various LTV sensitivities, the proposed VVO with DGs and different load models are more realistic and effective.

## V. CONCLUSION

In this paper, a MPC-based model for VVO dispatch based on forecasted DG outputs is proposed. The model considers exponential load models and the probabilistic nature of prediction errors of DG outputs and load consumptions. The VVO problem is formulated as a stochastic MINLP with the purposes to minimize power losses and feeder voltage deviations. Different types of customers (residential, commercial

and industrial customers) in a distribution system are taken into account by assigning corresponding exponents in the load models. Monte-Carlo simulations are run to generate scenarios of DG outputs. The MINLP is solved with reduced scenarios.

Case studies on the modified 33-bus test system with two wind turbines, one PV and different types of loads verify the effectiveness of the proposed VVO technique. The proposed VVO can reduce losses by up to 77% and reduce maximum voltage deviations by up to 65%. It should be noted that the stochastic MPC produces from two to three times greater benefits than the deterministic MPC approach. Finally, it appears that significant differences exist in VVO dispatches when load models are taken into account. Fig. 11 shows that using the exponential load model, the analysis estimates both active power losses and maximum voltage deviations to be lower compared to simulations using constant power loads. Compared with previous studies on VVO dispatch, the paper considers both improved load models and uncertain DG outputs. Thus, the proposed VVO model is more realistic and suitable to be used in practice.

## REFERENCES

- [1] T. Niknam, M. Zare, and J. Aghaei, "Scenario-based multiobjective volt/var control in distribution networks including renewable energy sources," *IEEE Trans. Power Del.*, vol. 27, no. 4, pp. 2004–2019, Oct. 2012.
- [2] Z. Wang and J. Wang, "Review on implementation and assessment of conservation voltage reduction," *IEEE Trans. Power Syst.*, vol. 29, no. 3, pp. 1306–1315, May 2014.
- [3] J. Grainger and S. Civanlar, "Volt/var control on distribution systems with lateral branches using shunt capacitors and voltage regulators Part I: The overall problem," *IEEE Trans. Power App. Syst.*, vol. PAS-104, no. 11, pp. 3278–3283, Nov. 1985.
- [4] B. A. De Souza and A. M. F. de Almeida, "Multiobjective optimization and fuzzy logic applied to planning of the volt/var problem in distributions systems," *IEEE Trans. Power Syst.*, vol. 25, no. 3, pp. 1274–1281, Aug. 2010.
- [5] R.-H. Liang and C.-K. Cheng, "Dispatch of main transformer ULTC and capacitors in a distribution system," *IEEE Trans. Power Del.*, vol. 16, no. 4, pp. 625–630, Oct. 2001.
- [6] J.-Y. Park, S.-R. Nam, and J.-K. Park, "Control of a ULTC considering the dispatch schedule of capacitors in a distribution system," *IEEE Trans. Power Syst.*, vol. 22, no. 2, pp. 755–761, May 2007.
- [7] G. W. Kim and K. Y. Lee, "Coordination control of ULTC transformer and STATCOM based on an artificial neural network," *IEEE Trans. Power Syst.*, vol. 20, no. 2, pp. 580–586, May 2005.
- [8] M. Singh, V. Khadkikar, A. Chandra, and R. K. Varma, "Grid interconnection of renewable energy sources at the distribution level with power-quality improvement features," *IEEE Trans. Power Del.*, vol. 26, no. 1, pp. 307–315, Jan. 2011.
- [9] F. A. Viawan and D. Karlsson, "Voltage and reactive power control in systems with synchronous machine-based distributed generation," *IEEE Trans. Power Del.*, vol. 23, no. 2, pp. 1079–1087, Apr. 2008.
- [10] F. A. Viawan and D. Karlsson, "Combined local and remote voltage and reactive power control in the presence of induction machine distributed generation," *IEEE Trans. Power Syst.*, vol. 22, no. 4, pp. 2003–2012, Nov. 2007.
- [11] T. Senjyu, Y. Miyazato, A. Yona, N. Urasaki, and T. Funabashi, "Optimal distribution voltage control and coordination with distributed generation," *IEEE Trans. Power Del.*, vol. 23, no. 2, pp. 1236–1242, Apr. 2008.
- [12] Y. P. Agalgaonkar, B. C. Pal, and R. A. Jabr, "Distribution voltage control considering the impact of PV generation on tap changers and autonomous regulators," *IEEE Trans. Power Syst.*, vol. 29, no. 1, pp. 182–192, Jan. 2014.
- [13] Z. Wang, B. Chen, J. Wang, and M. Begovic, "Inverter-less hybrid voltage/var control for distribution circuits with photovoltaic generators," *IEEE Trans. Smart Grid*, to be published.

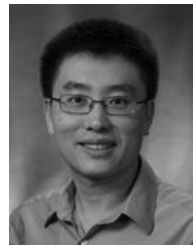
- [14] Y.-Y. Hong and Y.-F. Luo, "Optimal VAR control considering wind farms using probabilistic load-flow and gray-based genetic algorithms," *IEEE Trans. Power Del.*, vol. 24, no. 3, pp. 1441–1449, Jul. 2009.
- [15] J. V. Milanovic *et al.*, "International industry practice on power system load modeling," *IEEE Trans. Power Syst.*, vol. 28, no. 3, pp. 3038–3046, Aug. 2013.
- [16] P. Kundur, *Power System Stability and Control*. New York, NY, USA: McGraw-Hill, 1994.
- [17] D. Singh and K. Verma, "Multiobjective optimization for DG planning with load models," *IEEE Trans. Power Syst.*, vol. 24, no. 1, pp. 427–436, Feb. 2009.
- [18] J. Wen, Q. Wu, D. Turner, S. Cheng, and J. Fitch, "Optimal coordinated voltage control for power system voltage stability," *IEEE Trans. Power Syst.*, vol. 19, no. 2, pp. 1115–1122, May 2004.
- [19] C. Chen, W. Jianhui, H. Yeonsook, and S. Kishore, "MPC-based appliance scheduling for residential building energy management controller," *IEEE Trans. Smart Grid*, vol. 4, no. 3, pp. 1401–1410, Sep. 2013.
- [20] M. Moradzadeh, R. Boel, and L. Vandeveldel, "Voltage coordination in multi-area power systems via distributed model predictive control," *IEEE Trans. Power Syst.*, vol. 28, no. 1, pp. 513–521, Feb. 2013.
- [21] M. Larsson and D. Karlsson, "Coordinated system protection scheme against voltage collapse using heuristic search and predictive control," *IEEE Trans. Power Syst.*, vol. 18, no. 3, pp. 1001–1006, Aug. 2003.
- [22] M. Glavic, M. Hajian, W. Rosehart, and T. Van Cutsem, "Receding-horizon multi-step optimization to correct nonviable or unstable transmission voltages," *IEEE Trans. Power Syst.*, vol. 26, no. 3, pp. 1641–1650, Aug. 2011.
- [23] W. Price *et al.*, "Bibliography on load models for power flow and dynamic performance simulation," *IEEE Power Eng. Rev.*, vol. 15, no. 2, pp. 523–538, Feb. 1995.
- [24] H. Heitsch and W. Rörmisch, "Scenario reduction algorithms in stochastic programming," *Comput. Optim. Appl.*, vol. 24, nos. 2–3, pp. 187–206, Feb. 2003.
- [25] I. E. Grossmann, J. Viswanathan, A. Vecchiotti, R. Raman, and E. Kalvelagen, "GAMS/DICOPT: A discrete continuous optimization package," *Math. Methods Appl. Sci.*, vol. 24, no. 11, pp. 649–664, Jul. 2001.
- [26] M. E. Baran and F. F. Wu, "Network reconfiguration in distribution systems for loss reduction and load balancing," *IEEE Trans. Power Del.*, vol. 4, no. 2, pp. 1401–1407, Apr. 1989.
- [27] H.-G. Yeh, D. F. Gayme, and S. H. Low, "Adaptive VAR control for distribution circuits with photovoltaic generators," *IEEE Trans. Power Syst.*, vol. 27, no. 3, pp. 1656–1663, Aug. 2012.
- [28] M. Baran and F. F. Wu, "Optimal sizing of capacitors placed on a radial distribution system," *IEEE Trans. Power Del.*, vol. 4, no. 1, pp. 735–743, Jan. 1989.
- [29] K. Turitsyn, P. Sulc, S. Backhaus, and M. Chertkov, "Distributed control of reactive power flow in a radial distribution circuit with high photovoltaic penetration," in *Proc. IEEE Power Energy Soc. Gen. Meet.*, 2010, pp. 1–6.
- [30] R. J. Koessler, "Dynamic simulation of static VAR compensators in distribution systems," *IEEE Trans. Power Syst.*, vol. 7, no. 3, pp. 1285–1291, Aug. 1992.
- [31] H. Bludszuweit, J. A. Dominguez-Navarro, and A. Llombart, "Statistical analysis of wind power forecast error," *IEEE Trans. Power Syst.*, vol. 23, no. 3, pp. 983–991, Aug. 2008.
- [32] E. D. Castronuovo and J. P. Lopes, "On the optimization of the daily operation of a wind-hydro power plant," *IEEE Trans. Power Syst.*, vol. 19, no. 3, pp. 1599–1606, Aug. 2004.
- [33] A. Fabbri, T. G. S. Roman, J. R. Abbad, and V. M. Quezada, "Assessment of the cost associated with wind generation prediction errors in a liberalized electricity market," *IEEE Trans. Power Syst.*, vol. 20, no. 3, pp. 1440–1446, Aug. 2005.
- [34] L. Wu, M. Shahidepour, and T. Li, "Cost of reliability analysis based on stochastic unit commitment," *IEEE Trans. Power Syst.*, vol. 23, no. 3, pp. 1364–1374, Aug. 2008.



**Zhaoyu Wang** (S'13) received the B.S. and M.S. degrees in electrical engineering from Shanghai Jiaotong University, Shanghai, China, in 2009 and 2012, respectively, and the M.S. degree in electrical and computer engineering from the Georgia Institute of Technology, Atlanta, GA, USA, in 2012, where he is currently pursuing the Ph.D. degree from the School of Electrical and Computer Engineering.

In 2013, he joined the Decision and Information Sciences Division, Argonne National Laboratory, Argonne, IL, USA, as a Research Aide Intern.

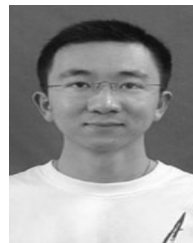
His research interests include microgrids, volt/var control, demand response and energy conservation, system modeling and identification, and stochastic optimization in power systems.



**Jianhui Wang** (M'07–SM'12) received the Ph.D. degree in electrical engineering from the Illinois Institute of Technology, Chicago, IL, USA, in 2007.

He is currently a Computational Engineer with the Decision and Information Sciences Division, Argonne National Laboratory, Argonne, IL. He is also an Affiliate Professor at Auburn University, Auburn, AL, USA, and an Adjunct Professor at the University of Notre Dame, Notre Dame, IN, USA.

Dr. Wang is a Chair of the IEEE Power and Energy Society (PES) Power System Operation Methods Subcommittee. He is an Editor of the IEEE TRANSACTIONS ON POWER SYSTEMS and the IEEE TRANSACTIONS ON SMART GRID, an Associate Editor of the *Journal of Energy Engineering*, an Editor of the IEEE PES LETTERS, an Associated Editor of *Applied Energy*, and an Editor of the Artech House Publishers Power Engineering Book Series. He is the recipient of the IEEE Chicago Section 2012 Outstanding Young Engineer Award.



**Bokan Chen** received the B.S. degree in electronics and information engineering from the Huazhong University of Science and Technology, Wuhan, China, in 2011, and the M.S. degree from the Department of Industrial and Manufacturing Systems Engineering, Iowa State University, Ames, IA, USA, where he is currently pursuing the Ph.D. degree in industrial engineering.

His research interests include optimization theories and their applications.



**Miroslav M. Begovic** (S'87–M'89–SM'92–F'04) received the B.S. and M.S. degrees in electrical engineering from Belgrade University, Belgrade, Serbia, in 1980 and 1985, respectively. He received the Ph.D. degree in electrical engineering from Virginia Polytechnic Institute and State University, Blacksburg, VA, USA, in 1989.

He is a Professor and Chair of the Electric Energy Technical Interest Group, School of Electrical and Computer Engineering, Georgia Institute of Technology, Atlanta, GA, USA. His research interests

include analysis, monitoring, control of voltage stability and applications of phasor measurements in electrical power systems, real-time monitoring systems for control of power system dynamics, protective relaying, distribution network operation, and distributed resources in energy systems.

Dr. Begovic was a Chair of the IEEE Power and Energy Society (PES) Emerging Technologies Coordinating Committee, and has contributed to technical activities within the IEEE and Conseil International des Grands Réseaux Électriques (CIGRE). He is a member of the IEEE PES Power System Relaying Committee and also a member of Sigma Xi, Tau Beta Pi, Phi Kappa Phi, and Eta Kappa Nu. He currently serves as a President of the IEEE Power and Energy Society.

**Yanyi He** received the B.S. degree in physics from the University of Science and Technology of China, Hefei, China, in 2007, and the M.S. degree in physics and the Ph.D. degree in industrial engineering from Iowa State University, Ames, IA, USA, in 2009 and 2013, respectively.

She is currently a Post-Doctoral Researcher at NEC Laboratories America, Inc., Cupertino, CA, USA. Her research interests include energy markets and energy managements.